2010

2M1938+4603: a rich, multimode pulsating sdB star with an eclipsing dM companion observed with Kepler

R H. Østensen

E. M. Green

S. Bloemen

T. R. Marsh

J. B. Laird

See next page for additional authors

Monthly Notices of the ROYAL ASTRONOMICAL SOCIETY LETTERS

Mon. Not. R. Astron. Soc. **408,** L51–L55 (2010) doi:10.1111/j.1745-3933.2010.00926.x

2M1938+4603: a rich, multimode pulsating sdB star with an eclipsing dM companion observed with *Kepler*

R. H. Østensen,[1⋆] E. M. Green,[2] S. Bloemen,[1] T. R. Marsh,[3] J. B. Laird,[2] M. Morris,[2] E. Moriyama,[2] R. Oreiro,[4] M. D. Reed,[5] S. D. Kawaler,[6] C. Aerts,[1,7] M. Vučković,[8] P. Degroote,[1] J. H. Telting,[9] H. Kjeldsen,[10] R. L. Gilliland,[11] J. Christensen-Dalsgaard,[10] W. J. Borucki[12] and D. Koch[12]

[1]*Instituut voor Sterrenkunde, K. U. Leuven, Celestijnenlaan 200D, 3001 Leuven, Belgium*
[2]*Steward Observatory, University of Arizona, 933 North Cherry Avenue, Tucson, AZ 85721, USA*
[3]*Department of Physics, University of Warwick, Coventry CV4 7AL*
[4]*Instituto de Astrofísica de Andalucía, Glorieta de la Astronomía s/n, 18008 Granada, Spain*
[5]*Department of Physics, Astronomy, and Materials Science, Missouri State University, Springfield, MO 65897, USA*
[6]*Department of Physics and Astronomy, Iowa State University, Ames, IA 50011, USA*
[7]*Department of Astrophysics, IMAPP, Radboud University Nijmegen, 6500 GL Nijmegen, the Netherlands*
[8]*European Southern Observatory, Alonso de Córdova 3107, Vitacura, Casilla 19001, Santiago, Chile*
[9]*Nordic Optical Telescope, 38700 Santa Cruz de La Palma, Spain*
[10]*Department of Physics and Astronomy, Aarhus University, 8000 Aarhus C, Denmark*
[11]*Space Telescope Science Institute, 3700 San Martin Drive, Baltimore, MD 21218, USA*
[12]*NASA Ames Research Center, MS 244-30, Moffett Field, CA 94035, USA*

Accepted 2010 July 28. Received 2010 July 28; in original form 2010 June 11

ABSTRACT

2M1938+4603 (KIC 9472174) displays a spectacular light curve dominated by a strong reflection effect and rather shallow, grazing eclipses. The orbital period is 0.126 d, the second longest period yet found for an eclipsing sdB+dM, but still close to the minimum 0.1-d period among such systems. The phase-folded *Kepler* light curve was used to detrend the orbital effects from the data set. The amplitude spectrum of the residual light curve reveals a rich collection of pulsation peaks spanning frequencies from ∼50 to 4500 μHz. The presence of a complex pulsation spectrum in both the p- and g-mode regions has never before been reported in a compact pulsator.

Eclipsing sdB+dM stars are very rare, with only seven systems known and only one with a pulsating primary. Pulsating stars in eclipsing binaries are especially important since they permit masses derived from seismological model fits to be cross-checked with orbital mass constraints. We present a first analysis of this star based on the *Kepler* 9.7-d commissioning light curve and extensive ground-based photometry and spectroscopy that allow us to set useful bounds on the system parameters. We derive a radial-velocity amplitude $K_1 = 65.7 \pm 0.6\,\mathrm{km\,s^{-1}}$, inclination angle $i = 69\overset{\circ}{.}45 \pm 0\overset{\circ}{.}20$, and find that the masses of the components are $M_1 = 0.48 \pm 0.03\,\mathrm{M}_\odot$ and $M_2 = 0.12 \pm 0.01\,\mathrm{M}_\odot$.

Key words: binaries: close – binaries: eclipsing – stars: individual: 2M1938+4603 – subdwarfs – stars: variables: general.

1 INTRODUCTION

The subdwarf B (sdB) stars are known to be core helium burning stars with extremely thin ($M_{\mathrm{env}} \leq 0.01\,\mathrm{M}_\odot$) inert hydrogen dominated envelopes (Heber 1986). This places them on an extension to the classical horizontal branch, known as the extreme horizontal branch (EHB). In order to reach this configuration, almost the entire envelope must be stripped off close to the tip of the red giant branch. There are several binary scenarios that are capable of accomplishing this, such as common-envelope ejection (CEE), stable Roche lobe overflow and merger of two helium-core white dwarfs (Han et al. 2002). A small minority of sdB stars in the field are found to have M-dwarf companions with periods of a few hours

⋆E-mail: roy@ster.kuleuven.be

(see For et al. 2010, for recent results and a review), and seven such systems are eclipsing. The eclipsing systems have been monitored over long time-bases in order to detect low-mass companions from precise measurements of the eclipse timings with the O − C method (Kilkenny, van Wyk & Marang 2003; Lee et al. 2009).

One of the eclipsing sdB+dM systems, NY Vir, has a pulsating primary of the V361 Hya class (Kilkenny et al. 1998). The V361 Hya stars were discovered by Kilkenny et al. (1997) and are characterized by rapid pulsations, typically in the period range between 2 and 5 min. They are known to be pressure (p-)mode pulsators excited by the κ mechanism, driven primarily by an iron opacity bump in the envelope (Charpinet et al. 1997). A second class of sdB pulsators was reported by Green et al. (2003). These stars, now known as V1093 Her stars, show pulsations with much longer periods (∼1 h) than the V361 Hya stars, and their temperatures are lower. These pulsations can be described in terms of gravity (g) modes excited by the same κ mechanism (Fontaine et al. 2003). With the discovery of long-period pulsations in a known rapid pulsator, DW Lyn, Schuh et al. (2006) established the existence of hybrid sdB pulsators. A broad review of hot subdwarf stars in general can be found in Heber (2009), and a review of asteroseismology and evolution of the EHB stars can be found in Østensen (2009). For the most recent ground-based pulsator discoveries see Østensen et al. (2010a).

The *Kepler* spacecraft was launched in 2009 March, aiming to find Earth-sized planets from photometric observations of a 105-deg^2 field (Borucki et al. 2010). *Kepler* is also ideally suited for asteroseismological studies, and the Kepler Asteroseismic Science Consortium (KASC; Gilliland et al. 2010) manages this important aspect of the mission. The methods with which the compact pulsator candidates were selected, together with analysis of the first half of the survey phase, are presented in Østensen et al. (2010b, hereafter Paper I). The first results on a V361 Hya star in the *Kepler* field are presented by Kawaler et al. (2010a), the first results on V1093 Her and DW Lyn pulsators are presented by Reed et al. (2010), and results on two V1093 Her pulsators in sdB+dM reflection binaries are discussed in Kawaler et al. (2010b). Further analysis of *Kepler* data on sdB stars are found in Van Grootel et al. (2010), which present the first detailed asteroseismic analysis of a V1093 Her star, and in Bloemen et al. (2010), which present a detailed analysis of the extraordinary binary light curve of the sdB+WD star KPD 1946+4340.

In this Letter we present 2M1938+4603 (KIC 9472174, g = 11.96), an object first identified as an sdB star in the *Kepler* field during a survey of blue targets selected from Two Micron All Sky Survey (2MASS) photometry. Follow-up photometry showed the presence of a reflection effect with shallow primary and secondary eclipses (Fig. 1). The amplitude of the reflection effect is very comparable to those observed in HW Vir and NY Vir, but the eclipses are much more shallow. After detrending the *Kepler* light curve, we clearly detect low-level pulsations.

2 OBSERVATIONS

The discovery of the strong reflection effect with grazing eclipses was made by two of us (JBL and MM) during a photometric run in 2008 June. Here we present only the eclipse timings from the ground-based photometry, as the pulsations are too complex and have too low amplitudes to be significant in those light curves. The times of 13 primary eclipses collected between 2008 June and 2010 May (Table S1) give the following ephemeris:

$$T_0 = 2454\,640.864\,162 \pm 0.000\,058\ \mathrm{d}$$
$$P = 0.125\,765\,300 \pm 0.000\,000\,021\ \mathrm{d}.$$

We downloaded the *Kepler* Q0 light curve from the KASC archive, corrected the raw time-stamps to Barycentric Julian Date (BJD) according to the instructions (Van Cleve 2009), and corrected the raw fluxes with a seventh-order polynomial to take out trends on time-scales longer than a day. The 77 consecutive eclipse times measured from the *Kepler* photometry (Table S2) match the ground-based ephemeris well within the errors. Both the ground- and space-based eclipse times are provided in the on-line supplement.

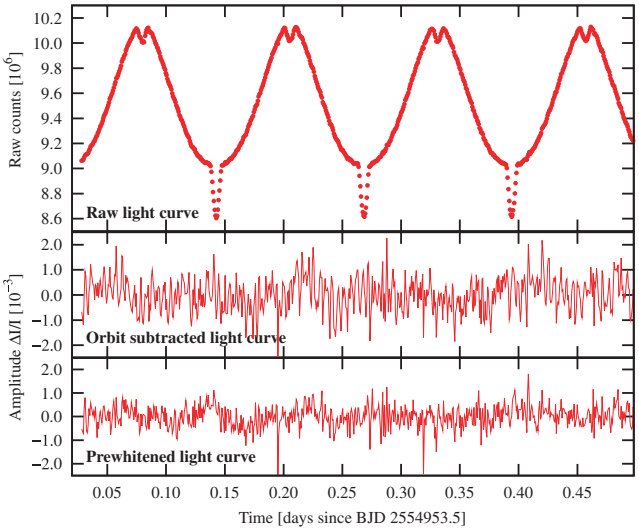

Figure 1. The first half day of the *Kepler* light curve. The upper panel shows the raw data, which are dominated by the strong reflection effect, with both primary and secondary eclipses clearly visible. The middle panel shows the same chunk after detrending with the light curve folded on P, and the bottom panel shows the same after prewhitening the 55 most significant frequencies.

In order to produce a useful Fourier transform (FT) that shows the spectrum of low-level pulsations in 2M1938+4603 among the extremely dominant orbital effects (Fig. 1, top panel) we first attempted to clean out a model light curve of the system (see Section 3), but we abandoned this approach since the FT of the residuals contain significant peaks at *every* orbital harmonic. The model light curve is unable to produce a satisfactory fit to the complicated irradiation effect, at the exceptional precision of the *Kepler* photometry. Our model light curve does not account for radiative transfer through the heated face of the M-dwarf, which may account for some of the discrepancies between the model and data. Until such issues are resolved the precise parameters of our model are subject to systematic uncertainties that could well be in excess of the statistical errors. Even if we managed to model all orbital effects in the light curve to the required precision, any pulsation peaks found in the residuals on an orbital harmonic frequency would still be suspicious. So instead we proceeded by folding the *Kepler* light curve on P, and then using the result to clean out all orbital effects from the light curve. Note that any stable pulsations that coincide with harmonics of the orbital period within the resolution are also very effectively removed.

2.1 Frequency determination

After removing the orbital effects from the light curve, a spectacularly rich pulsation spectrum is revealed (upper half of the five

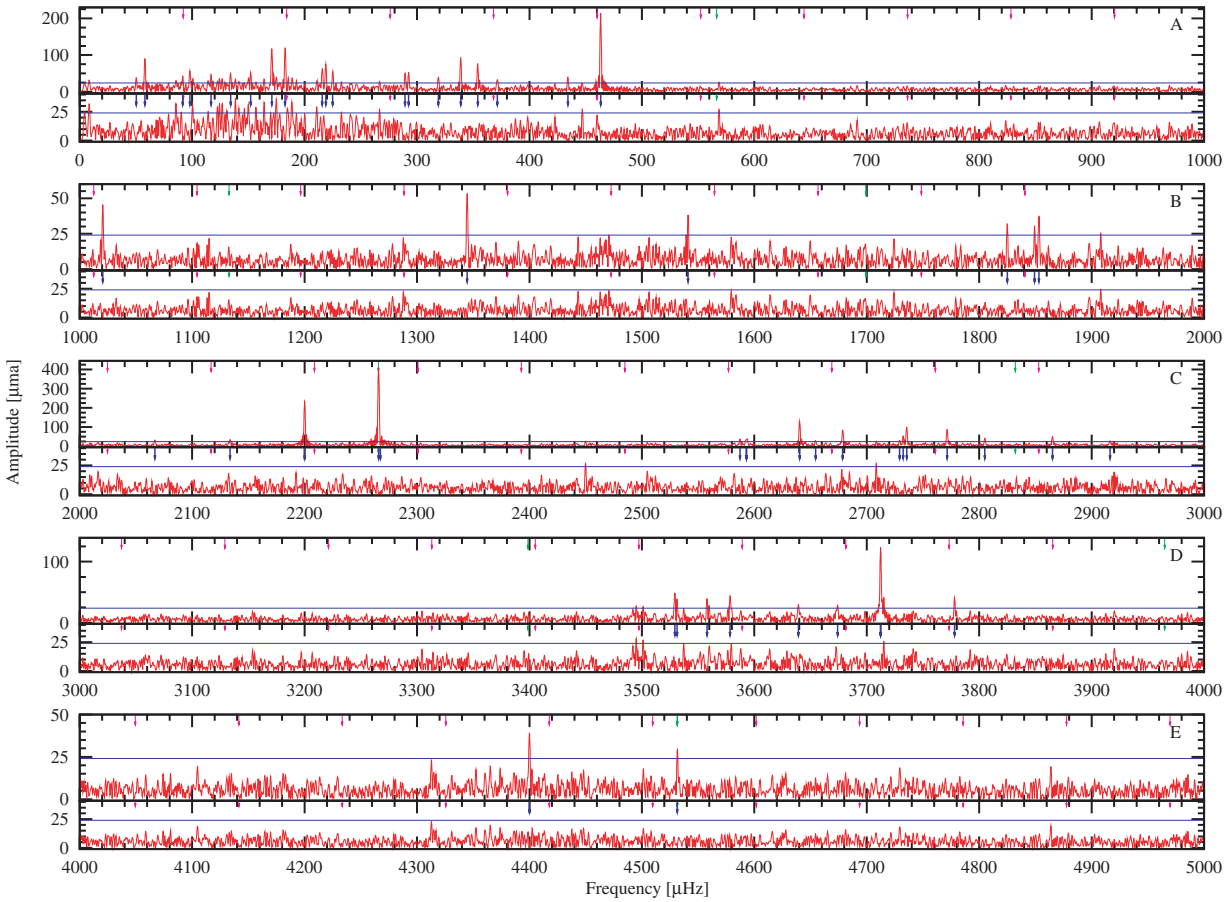

Figure 2. The FT of the data after detrending the orbital and long-term variations (upper part of each panel). The panels are labelled A, B, C, D, E which also define the group designation used in Table S4. The magenta arrows indicate the orbital frequency of $f_{\rm orb} = 92$ μHz and all its harmonics. The green arrows indicate the *Kepler* long-cadence cycle, $f_{\rm lc}$, and its harmonics, at which possible artefacts are known to be found. The lower part of each panel shows the FT of the data after prewhitening 55 frequencies, as marked with blue arrows. The blue line indicates four times the mean noise level at 24 μma.

panels in Fig. 2). We have identified 55 frequencies between ∼50 and 4500 μHz that have amplitudes well above four times the mean level of 6 μma[1] computed from the whole FT between 500 μHz and the Nyquist frequency, $f_{\rm Nyq} = 8496$ μHz. The frequency list is provided in Table S4. Several more frequencies remain above the 24-μma limit, after prewhitening the light curve with these 55 frequencies (lower half of the panels in Fig. 2), especially in the low-frequency region below 500 μHz. However, we chose to constrain ourselves to the most clearly resolved peaks in this first analysis, as much more *Kepler* data are underway, and will provide a 10-fold increase in resolution and a threefold drop in the noise level after only the first three-month cycle of observations. In total we hope to obtain close to 5 yr of almost continuous space-based observations on this object, so we will limit ourselves to discussing only the most obvious features here.

The FT shows several distinct groups of frequencies, and we number the frequencies in each group separately as A, B, C, D, E as indicated in Fig. 2. The frequencies in group A are typical for the V1093 Her stars, and we identify and remove 20 peaks, with the lowest at 6σ. There are clearly many more frequencies than this, in particular between 100 and 200 μHz, but the resolution is not good enough to justify pushing the limit further. There are no significant frequencies between 500 and 1000 μHz, except one at 570 μHz which is just above the detection limit. Note also that this frequency is close to the long-cadence readout cycle at $f_{\rm lc} = 566.4$ μHz. In group B we find only six rather low-level peaks. Group C contains the strongest peak in the FT at $f_{\rm C4} = 2265.8$ μHz with an amplitude of 423 μma. This frequency is almost exactly at $4f_{\rm lc} = 2265.4$ μHz, but since we do not observe such strong artefacts in any other stars we are inclined to believe that this is a real pulsation mode. In all other short-cadence *Kepler* data sets we have worked with, the strongest artefact peak is found at 8 or $9f_{\rm lc}$. In this data set $9f_{\rm lc}$ is not present at all, and $8f_{\rm lc} = 4531$ μHz is barely above the detection limit, while $f_{\rm C4}$ is 70σ. The second strongest peak in the FT is also found right next to it, $f_{\rm C3} = 2200.1$ μHz with an amplitude of 233 μma. Another rich set of peaks is found around 2700 μHz, so that group C contains 18 peaks altogether. Group D contains nine clear peaks between 3500 and 3800 μHz, and group E contains only two significant peaks located at $2f_{\rm C3}$ and $2f_{\rm C4} = 8f_{\rm lc}$.

The frequency analysis and error estimations on the parameters are done as outlined in Degroote et al. (2009). Because some of the frequencies were unresolved, we have performed additional analysis, where after each prewhitening stage, some of the frequencies, amplitudes and phases were refitted with a Levenberg–Marquardt non-linear fitting routine. To investigate the stability of the fit and the

[1] One micromodulation amplitude (μma) is equivalent to a semi-amplitude of 1 part per million of the mean light level.

differences from the linear analysis, we first only updated the amplitudes, phases and frequencies belonging to the last two identified peaks, then updating the parameters belonging to the last 20 peaks, and finally using all identified frequencies. The differences between the amplitudes and frequencies were all within the derived error estimates, except for the frequencies around 3712 and 2593 μHz. The non-linear fitting algorithm did not produce consistent results at these frequencies, but future observations will allow us to resolve these structures. Below 200 μHz, a dense forest of barely significant peaks is visible. Although the different methods give mostly consistent results, more *Kepler* photometry will be necessary to fully resolve them.

2.2 Spectroscopy

Spectroscopic observations to determine radial velocities for 2M1938+4603 were undertaken primarily with the B&C spectrograph on the 2.3-m *Bok Telescope* on Kitt Peak. A few spectra were also obtained using the MMT Blue spectrograph. In both cases, an 832 lines mm^{-1} grating was employed in second order, and particular care was taken to maintain precise centring of the star on the slit throughout the exposures. The resulting spectra have a resolution of $R \sim 2150$ over the range 3675–4520 Å (Bok), or $R \sim 4200$, 4000–4950 Å (MMT). Radial velocities were derived by cross-correlating the individual continuum-removed spectra against a supertemplate using the IRAF task FXCOR. The supertemplate for the lower resolution spectra was obtained by shifting the 66 individual spectra to the same velocity prior to median filtering into a single spectrum; the velocity zero-point of the resulting template was thus undetermined. The cross-correlation template for the six MMT spectra was constructed from 19 spectra previously obtained with the identical spectroscopic set-up for other hot subdwarfs of known radial velocities, whose spectral abundance patterns closely match that of 2M1938+4603.

A single sinusoidal fit was performed to all 72 velocities as a function of orbital phase, weighted by the velocity errors and also including an additional term for the zero-point offset of the Bok velocities relative to the MMT velocities (Fig. 3). The orbital period was fixed at the value of 0.125 760 d derived from the eclipse timings. The derived radial velocity (RV) semi-amplitude is $K_1 = 65.7 \pm 0.6\,km\,s^{-1}$, with a systemic velocity $\gamma = 20.1 \pm 0.3\,km\,s^{-1}$.

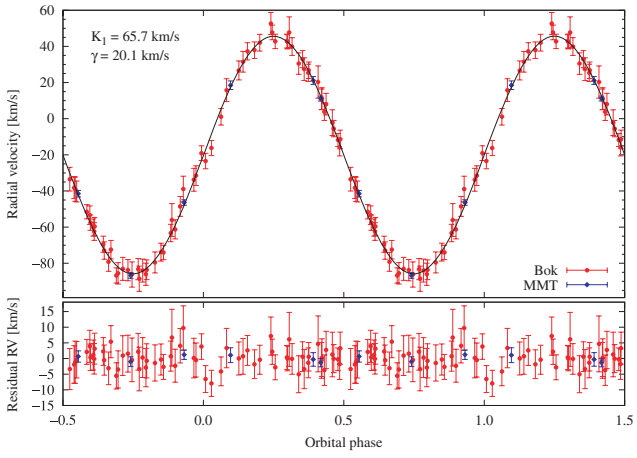

Figure 3. RV data from the Bok and MMT telescopes (Table S3), with the best-fitting solution as a sine curve (top), and the residuals (bottom).

3 SYSTEM PARAMETERS

The effective temperature, surface gravity and helium abundance of 2M1938+4603 were determined in the context of Paper I to be $T_{\rm eff} = 29\,564 \pm 106$ K, $\log g = 5.425 \pm 0.009$ dex and $\log(N_{\rm He}/N_{\rm H}) = -2.36 \pm 0.06$ dex, using metal blanketed local thermodynamic equilibrium (LTE) models. This temperature is close to the boundary region between the p- and g-mode pulsators, where hybrid DW Lyn type pulsators have been found.

We modelled the light curve using grid elements covering each star, accounting for tidal (ellipsoidal) distortion of each star and gravity and limb darkening of the sdB as in Bloemen et al. (2010). Irradiation of the M-dwarf was accounted for by summing the M-dwarf flux with the incident flux from the sdB point by point. Surface brightnesses were computed assuming blackbody spectra at a single wavelength of 600 nm. The best-fitting model is found to have the following parameters: inclination angle, $i = 69.^{\circ}45(2)$, relative radii, $r_1 = 0.250(1)$, $r_2 = 0.177(1)$ in units of the orbital separation. The errors in parentheses are formal fitting errors that may underestimate the true errors perhaps as much as a factor of 10, considering the discrepancies in the light-curve fitting. The high precision on these parameters allows us to use the mass–radius relationships as derived from the orbital parameters and from the surface gravity to constrain the mass and radius of the primary, as shown in Fig. 4. We clearly see that the permitted M, R given by the photometric orbital parameters (P, i, r_1 and r_2) and the spectroscopic K_1 crosses the M, R given by the spectroscopic surface gravity at precisely the expected primary mass for a post-CE sdB star. The adjacent dotted lines indicate the errors (on the RV for the q-track and on $\log g$ for the g-track since the errors on P, i and the relative radii are too small to matter). A mass for the primary of $M_1 = 0.48 \pm 0.03\,M_\odot$ can be deduced from the diagram. Using K_1 and P we know the mass function $f(M) = 0.003\,695$. With $0.48\,M_\odot$ for the primary, and solving for the secondary, we get $M_2 = 0.12 \pm 0.01\,M_\odot$.

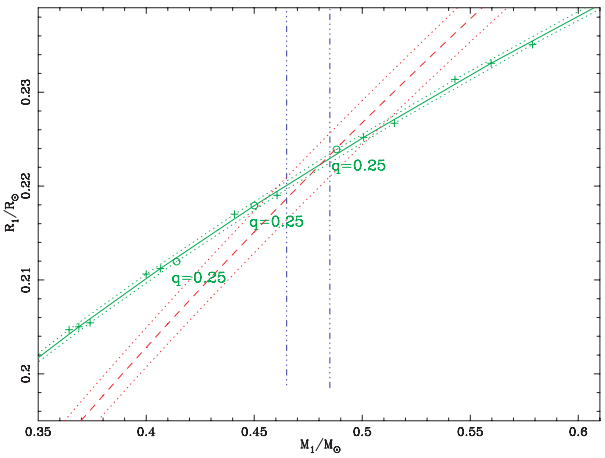

Figure 4. Mass–radius diagram showing the regions permitted by the orbit (green) and by the spectroscopic gravity (red). The green-dotted curves show the error ranges that correspond to a 3σ error in K_1. The red-dotted curves correspond to the 1σ formal error on $\log g$ for the gravity track. The green curves are labelled with the value for $q = M_1/M_2$ that corresponds to each point on the curve, with ticks of 0.01, increasing to the left-hand side. Note that changing K_1 by 3σ shifts the curve very little in the M/R plane, but the q-value changes considerably. Vertical lines show the mass range typical for EHB stars formed through the CE channel.

4 DISCUSSION AND OUTLOOK

We have presented the discovery of a new eclipsing sdB with an M-dwarf companion, and demonstrated that the primary is an unusual pulsator with frequencies spanning the range from 50 to 4400 μHz. The unprecedented precision of the *Kepler* observations makes a direct comparison to other known eclipsing sdB+dM systems rather difficult, since such low-level pulsations as we find in 2M1938+4603 would be undetectable from the ground. Nevertheless, it is an amazing stroke of luck to find an eclipsing sdB+dM system within the narrow confines of the *Kepler* field, especially one as bright as $g = 11.96$, considering the fact that only seven eclipsing systems are known among the thousands of subdwarfs that have been surveyed for variability to date.

In future papers we will produce a more realistic model that can handle the irradiation effect of the M-dwarf to improve the binary light-curve model, and produce asteroseismic models that can reproduce the frequencies observed in this star. When longer time series of *Kepler* photometry become available, we will be able to fully resolve the densely packed amplitude spectrum that we see in the g-mode region between 100 and 200 μHz. This will enable us to produce an asteroseismic model reproducing all the frequencies in this complex rotating pulsator, as was done for NY Vir by Charpinet et al. (2008). Since 2M1938+4603 has g modes in addition to p modes we should also be able to constrain the deeper structure of the sdB core, and hopefully also establish the mass of its progenitor, before the envelope was ejected by the companion. With 5 yr of precise eclipse timings we may detect planetary companions from variations in the O − C diagram, if they orbit this compact binary with periods shorter than the *Kepler Mission*. If the low-amplitude pulsations are found to be stable on such time-scales, pulsation timing can be used to confirm the period, thereby eliminating any ambiguity of the detection.

ACKNOWLEDGMENTS

The authors gratefully thank the *Kepler* team and all who contributed to making the mission possible. The *Kepler Mission* is funded by NASA's Science Mission Directorate.

We acknowledge funding from the European Research Council under the Seventh Framework Programme (ERC/FP7 No. 227224, PROSPERITY), as well as from the Research Council of K. U. Leuven (GOA/2008/04).

REFERENCES

Bloemen S. et al., 2010, MNRAS, in press
Borucki W. J. et al., 2010, Sci, 327, 977
Charpinet S., Fontaine G., Brassard P., Chayer P., Rogers F. J., Iglesias C. A., Dorman B., 1997, ApJ, 483, L123
Charpinet S., van Grootel V., Reese D., Fontaine G., Green E. M., Brassard P., Chayer P., 2008, A&A, 489, 377
Degroote P. et al., 2009, A&A, 506, 471
Fontaine G., Brassard P., Charpinet S., Green E. M., Chayer P., Billères M., Randall S. K., 2003, ApJ, 597, 518
For B.-Q. et al., 2010, ApJ, 708, 253
Gilliland R. L. et al., 2010, PASP, 122, 131
Green E. M. et al., 2003, ApJ, 583, L31
Han Z., Podsiadlowski P., Maxted P. F. L., Marsh T. R., Ivanova N., 2002, MNRAS, 336, 449
Heber U., 1986, A&A, 155, 33
Heber U., 2009, ARA&A, 47, 211
Kawaler S. D. et al., 2010a, MNRAS, in press (arXiv:1008.2356)
Kawaler S. D. et al., 2010b, MNRAS, in press (arXiv:1008.0553)
Kilkenny D., Koen C., O'Donoghue D., Stobie R. S., 1997, MNRAS, 285, 640
Kilkenny D., O'Donoghue D., Koen C., Lynas-Gray A. E., van Wyk F., 1998, MNRAS, 296, 329
Kilkenny D., van Wyk F., Marang F., 2003, The Observatory, 123, 31
Lee J. W., Kim S.-L., Kim C.-H., Koch R. H., Lee C.-U., Kim H.-I., Park J.-H., 2009, AJ, 137, 3181
Østensen R. H., 2009, Communications Asteroseismology, 159, 75
Østensen R. H. et al., 2010a, A&A, 513, A6
Østensen R. H. et al., 2010b, MNRAS, in press (arXiv:1007.3170)
Reed M. et al., 2010, MNRAS, in press (arXiv:1008.0582)
Schuh S., Huber J., Dreizler S., Heber U., O'Toole S. J., Green E. M., Fontaine G., 2006, A&A, 445, L31
Van Cleve J. E., 2009, Kepler Data Release Notes 2, http://archive.stsci.edu/kepler/release_notes/release_notes2/Data_Release_02_Notes_2009102213.pdf
Van Grootel V. et al., 2010, ApJ, 718, L97

SUPPORTING INFORMATION

Additional Supporting Information may be found in the online version of this article:

Table S1. Primary minima from ground-based data.
Table S2. Primary minima from *Kepler* data.
Table S3. RV measurements.
Table S4. Frequencies, periods and amplitudes.

Please note: Wiley-Blackwell are not responsible for the content or functionality of any supporting materials supplied by the authors. Any queries (other than missing material) should be directed to the corresponding author for the article.

This paper has been typeset from a TEX/LATEX file prepared by the author.